Journal of Arid Environments (2002) **52**: 305–317
doi:10.1006/jare.2002.1006, available online at http://www.idealibrary.com on IDEAL®

Surface mosaic map unit development for a desert pavement surface

Yvonne A. Wood★*, Robert C. Graham★ & Stephen G. Wells†

★*Soil and Water Sciences Program, Department of Environmental Sciences, University of California, Riverside, CA 92521, U.S.A.*
†Desert Research Institute, Reno, NV 89506, U.S.A.

(Received 10 January 2001, accepted 25 February 2002)

Desert pavement plays a fundamental role in arid land processes. The first step towards quantitatively analysing this role is detailed surficial mapping. To this end, map units were developed to represent the physical variability of a desert pavement surface at a large scale (decimeters to meters). Six distinct map units were defined by surface textural parameters of clast size, percent cover, and sorting through fieldwork on a basalt flow in the Mojave Desert. These surface mosaics abut with visually distinct boundaries and are easily identified in the field. Field reconnaissance showed that delineation into such units is applicable to the detailed study of other desert pavement surfaces.

Keywords: stone mantle; spatial heterogeneity; ecological patchiness; surficial mapping; grain size; median diameter; sorting; clast cover

Introduction

In North America, about 50% of the desert land surface is desert pavement (Evenari, 1985), a feature composed of closely packed clasts, one to two deep, resting on or embedded in soils several centimeters to meters thick (Springer, 1958; Cooke, 1965, 1970; Hunt & Mabey, 1966). Desert pavement mantles gently sloping landforms including alluvial fans, basalt flows, pluvial lake benches, and ancient alluvial terraces (Cooke *et al.*, 1993). Wherever found it plays a fundamental role in geomorphic, hydrologic, pedologic, and ecosystem processes (Wells *et al.*, 1985; McFadden *et al.*, 1987; Abrahams & Parsons, 1991; Cooke *et al.*, 1993; Dunkerley & Brown, 1995; Smith *et al.*, 1995). 'Desert varnish', a hard, dark patina from the accumulation of iron and manganese oxides, usually covers the surface of the clasts (Whalley, 1983). From afar, desert pavement makes hillslopes and flats with scant vegetation appear darkly polished, while up close, it appears as a carefully constructed cobblestone surface.

At a landscape scale, clumps of desert shrubs on bare soil, surrounded by wide expanses of nearly planar desert pavement (Fig. 1), alter the flow of wind and water as

*Corresponding author. Fax: +1-909-686-8942

Figure 1. Typical view of spatially heterogeneous desert pavement surface on the 560 ka basalt flow in the Cima volcanic field, eastern Mojave Desert, California. Note expanses of well-developed desert pavement surrounding 'islands' of desert scrub and bare ground in the middle of the photograph. Field of view across bottom of photograph is approximately 2 m.

well as rates of infiltration and runoff, in spatially disjunct patterns (Abraham & Parsons, 1991; Dunkerley & Brown, 1995). At a large scale (decimeters to meters), the physical character of the desert pavement soil surface is spatially complex, varying from high percent clast cover and close packing through moderate cover to near absence of clasts (Denny, 1965; Hunt & Mabey, 1966; McFadden *et al.*, 1989). Accurate mapping of this spatial complexity is an important step in the study of desert pavement surficial processes. In this work, surface physical differences were described and quantified based on detailed field measurements of a desert pavement formed on a basalt flow in the Mojave Desert of California.

Methods

Surficial mapping techniques were used to develop six mapping units named surface mosaics which accurately and consistently classified the dominant surface types of the field site when observed at a large scale (one to tens of meters). These surface mosaics were characterized in detail and tested for consistency across the landform (Compton, 1985). Surface clast size, percent cover, and sorting were characteristics found to accurately differentiate surface mosaics.

Study site

Work was conducted on a desert pavement mantling a 560 ka basalt flow (Turrin *et al.*, 1985) in the Cima Volcanic Field of the eastern Mojave Desert, California (Fig. 2). This Pliocene to Holocene field is comprised of ~40 cinder cones and more than 60 associated basalt flows. The chosen basalt flow, mapped as e1 by Dohrenwend *et al.* (1984), was selected because of its known age, well-developed desert pavement, and past extensive research (Dohrenwend *et al.*, 1987; Farr, 1992; Arvidson *et al.*, 1993), including development of the eolian deposition model of desert pavement formation (Wells *et al.*, 1985, 1995; McFadden *et al.*, 1986, 1987).

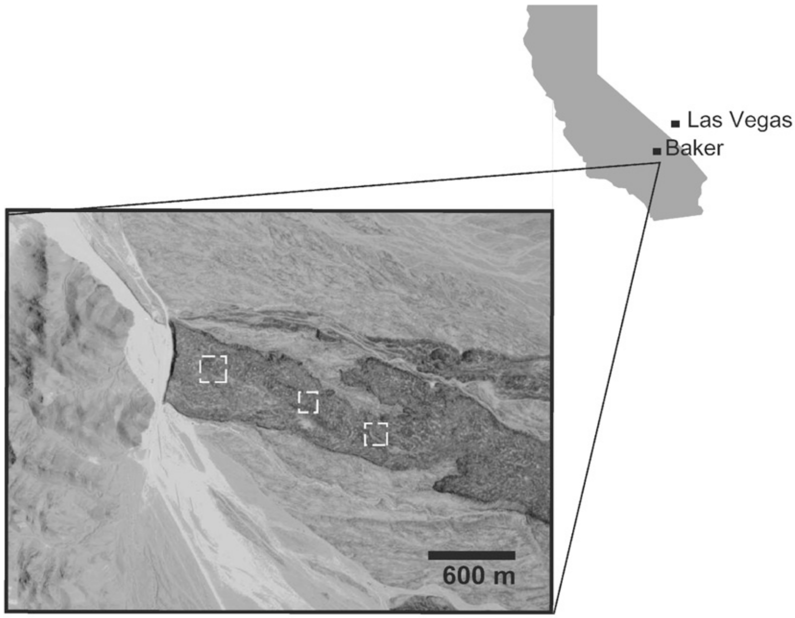

Figure 2. Location of study site. Vertical aerial photograph shows location of sampling plots on the surface of the 560 ka basalt flow of the Cima volcanic field, eastern Mojave Desert, California. Dark area is basalt flow with surrounding light alluvial fan and wash deposits. Road is vertically trending, narrow white line in the left half of the photograph.

The study site is at an elevation of 700 m, approximately 22 km south of Baker, California, and 150 km southeast of Las Vegas, Nevada. The climate is arid and hot with primarily winter precipitation. Using data from nearby weather stations, mean annual precipitation is calculated to be 70 mm, and mean annual air temperature to be 17°C (NOAA, 1999). Plant cover is perennial creosote (*Larrea tridentata*) scrub associations (Billings, 1949; Vasek & Barbour, 1988) with primarily winter annuals (Ludwig *et al.*, 1988). Soils are Aridisols formed in quartz-rich desert loess comprised of well-sorted sandy silts (McFadden *et al.*, 1986). The surface soil horizon is usually a vesicular, clay-enriched, thin platy crust often referred to as the Av horizon (Jackson, 1957; Nettleton & Peterson, 1983; McFadden *et al.*, 1987, 1998). Clays and salts have accumulated beneath the Av horizon, promoting the formation of strong coarse plates and columns (McFadden *et al.*, 1987).

Sampling

A sampling location far removed from evidence of foot or vehicular travel was selected. Preliminary characterization of the surface was done using three randomly selected 30-m tape transects and included determination of clast size distributions and percent cover. For each meter increment of a 30-m tape, surface clasts touching the tape were categorized by the following: (1) size distributions of large (> 150 mm), medium (64–150 mm), small (10–64 mm), and very small (< 10 mm); (2) rounding class (Compton, 1985); and (3) embedding into the soil (measured by ability to easily dislodge clasts by one hand). Percent clast cover was estimated using percentage diagrams (Compton, 1985, pp. 366–367) for a meter-wide belt along the 30-m tape, again for each meter increment of the tape.

Recorded percent cover values were used to define preliminary map units (Fig. 3). Desert pavement regions are visually distinct from the bare ground regions and consistently had percent clast cover values of greater than 65%. Separate cluster analyses (Data Description, Inc., 1995) of percent cover values for desert pavement (>65%) and for bare ground (<65%) regions identified five preliminary map units (Fig. 3).

Plan view photos were taken of representative map unit surfaces at the sampling location and used for preliminary field mapping. During this phase one bare ground map unit was divided into two units based on visual differences in clast size sorting. Additionally, the visually distinct boundaries between map units were categorized based on the distance through which one mosaic grades into another as follows: very sharp (⩽10 mm), sharp (10–30 mm), gradual (30–100 mm), and diffuse (>100 mm).

Six volunteers (including scientists and non-scientists) were asked to use photographs of the resulting six surface mosaics to identify them in the field. This assured that correct assignments of surface mosaic types could be done by others, and that the map units fit Compton's (1985, p. 83) requirement that they are "obvious, natural and suit the scale of the map".

To provide detailed characterization of the six surface mosaics, 1-m line transects were completed near the original type locality for each map unit recording the length (*a*-axis) and width (*b*-axis) for each clast touched by the line. To test the consistency of these map units across the land's surface, two additional sampling locations were established at least 500 m distant from the first location on the same basalt flow (Fig. 2). At these two sampling locations additional detailed 1-m long line transects were completed, providing triplicate measurements for each defined map unit surface type.

Statistical analyses

Standard sedimentological values (Folk, 1980) were calculated for the data collected from the triplicate meter transects. Verbal designations of clast size classes were

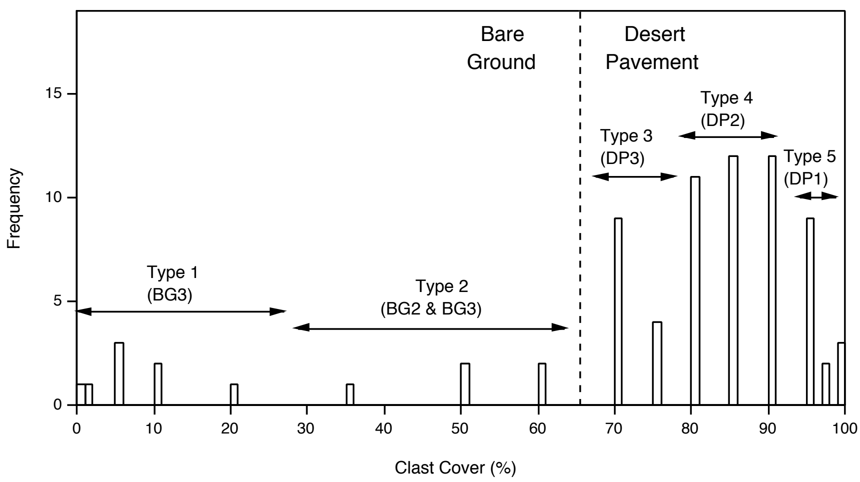

Figure 3. Histogram showing clast percent cover values from the study site as measured using one meter increments along three 30-m line transects. As shown by the arrows, five preliminary surface types were differentiated based on cluster analysis (Data Description, Inc., 1995) of these data. These were later named as indicated in parentheses.

assigned using the USDA scale (Schoenberger *et al.*, 1998). This scale relies on clast length and has the following divisions: fine gravel (2–5 mm), medium gravel (5–20 mm), coarse gravel (20–75 mm), cobbles (75–250 mm), stones (250–600 mm), and boulders (> 600 mm). Analysis of variance (ANOVA) and Tukey's studentized range test were performed to compare the resulting clast size distributions. Additionally, values representing the sedimentological moments of mid-point and sorting (Folk, 1980) for each defined surface mosaic were analysed using three-dimensional cluster analysis (Data Description, Inc., 1995) to assure their consistency across the study site.

Results

The overall surficial patterning of the study site is one of desert pavement surrounding polygons of bare ground (Fig. 1). Within these two broad categories are found six visually distinct surface mosaics arrayed in a heterogeneous pattern (Fig. 4) which are easily identified using surface clast characteristics (Table 1) of (a) percent cover, (b) median size (*b*-axis), and (c) degree of sorting (as a measure of clast size uniformity). The six surface mosaics are defined as DP1, DP2, and DP3 (desert pavement surface mosaics with clast cover of greater than 65%), and BG1, BG2, and BG3 (bare ground surface mosaics with clast cover less than 65%). Plan view photographs of the six surface mosaics (Fig. 5) illustrate their visual differences. Using these photographs, the six volunteers could readily identify the surface mosaics across a wide area of the study site. Calculated sedimentologic parameters (Folk, 1980) indicate the significant differences between the clast size distributions of the surface mosaics (Table 1).

Desert pavement (DP) surface mosaics

Surface mosaics DP1, DP2, and DP3 define areas for which closely packed clasts as desert pavement predominate. Measured physical characteristics within each desert

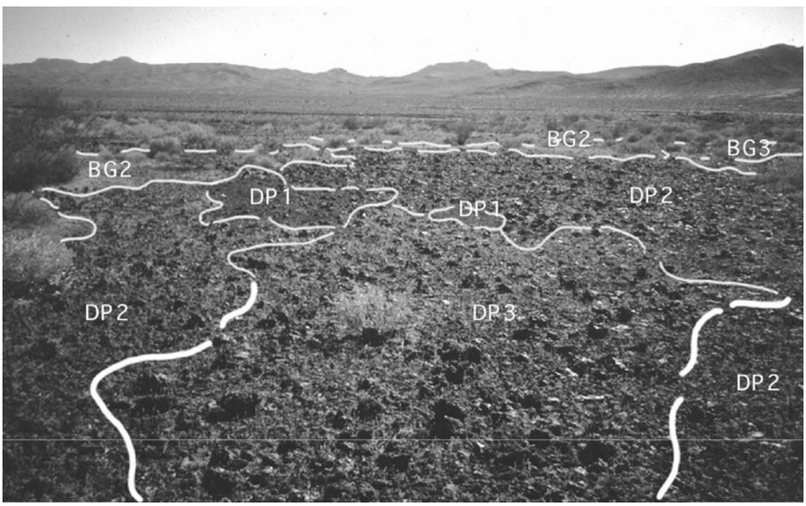

Figure 4. Delineation of desert pavement land surface at the study site into surface mosaic map units defined by physical characteristics of median clast size, sorting index, and clast cover as indicated in Table 1. These delineations can be transferred onto topographic maps for later use in large-scale statistical analyses.

Table 1. *Sedimentological data for surface mosaic map units from triplicate 1-m transects measured on the desert pavement land surface of a 560 ka basalt flow in the Cima volcanic field, east Mojave Desert, California. All calculated values use b-axis diameters*★

Mosaic	Clast cover (%)	Sorting†	Clast width‡ (mm)					Clast frequency ($N\,m^{-1}$)	Clast form§¶	Clast rounding§‖	Clast position§★★	Mosaic boundary††
			Median	Mean	Mode	Maximum	Minimum					
Desert pavement												
DP1	95 (0)	0·8 (0·0)	8 (1)	12 (1)	7 (2)	66 (39)	2 (1)	72 (5)	E/P	SA	Lo	Very sharp
DP2	87 (4)	1·3 (0·2)	12 (0)	22 (2)	9 (3)	107 (30)	2 (0)	48 (4)	E/P	SA	Lo	Sharp
DP3	69 (4)	1·3 (0·2)	36 (9)	45 (6)	49 (25)	111 (9)	7 (3)	18 (3)	E/P	SR	Em+	Sharp
Bare ground												
BG1	54 (12)	1·4 (0·2)	22 (7)	36 (10)	30 (21)	131 (62)	5 (1)	13 (3)	P	SA	Lo	Diffuse
BG2	58 (9)	1·2 (0·3)	17 (3)	27 (6)	16 (4)	82 (35)	3 (1)	23 (5)	P	SA	Lo	Gradual
BG3	21 (7)	1·3 (0·2)	30 (6)	40 (7)	NA	93 (38)	9 (5)	8 (5)	P	SR	Em+	Gradual

★Values reported are the mean of triplicate detailed 1-m transects. Standard error values (±) are given in parentheses.
†Values indicate how closely clasts approach being one size (Compton, 1985). Here, values above 1 indicate poorly sorted and below 1 indicate moderately sorted (Folk, 1980). For comparison, beach sands are usually very well sorted (with values of ~0·3) and glacial tills are extremely poorly sorted (values >4).
‡Based on width (*b*-axis diameters) of surface clasts.
§Clasts with widths of approximately the median diameter were used to assign these qualitative values (Folk, 1980).
¶E = equidimensional; P = platy (Folk, 1980).
‖SA = subangular; SR = subrounded (Compton, 1980; Schoenenberger, 1998).
★★Lo = loose (resting on top of surface); Em = embedded (easily removed from soil surface with one hand); Em+ = tightly embedded (requires strength of at least both hands to remove from soil surface).
††Very sharp (⩽10 mm width); sharp (between 10 and 30 mm); diffuse (3/4 100 mm); gradual (>100 mm). These boundaries reflect the edge of the specific mosaic type. When using for field descriptions of the boundary between mosaics, revert to the nomes for the widest observed boundary.

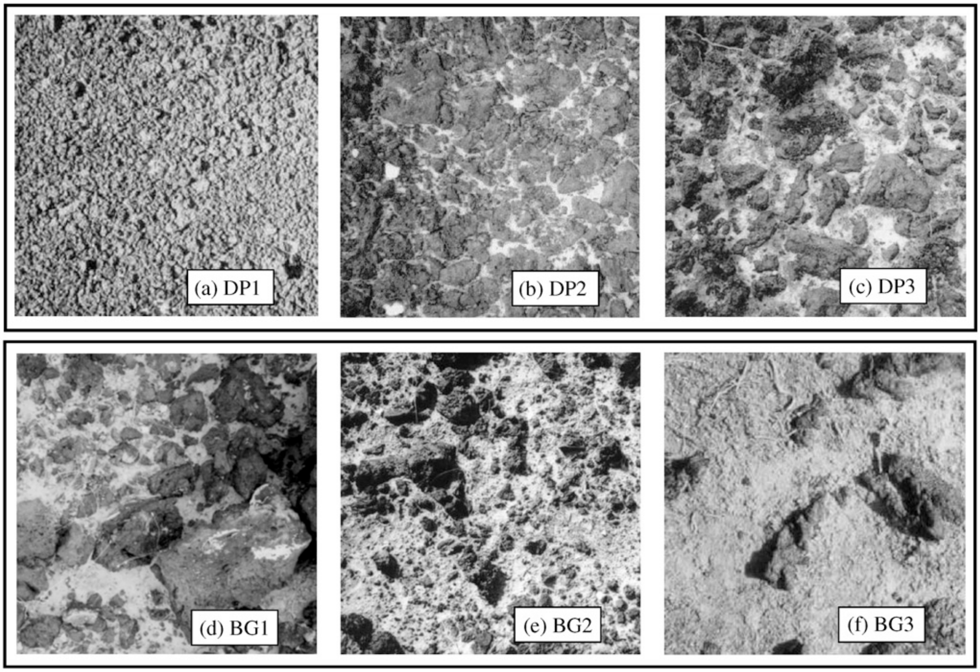

Figure 5. Plan view photographs of the six defined and tested surface mosaics. Field of view of each photograph is 50 cm. Physical characteristics of these mosaics are summarized in Table 1.

pavement surface mosaic are unique and vary discretely (Tables 2 and 3) with sharp boundaries (Table 1) between defined map units. While surface mosaics DP1 and DP2 have the same clast width mode (7–9 mm), their mean widths differ by a factor of two (12 as compared to 22 mm), reflecting different clast size distributions (Table 1). These two distributions differ significantly from those of DP3, which has nearly identical values for its mode (49 mm) and mean (45 mm) widths.

Surface mosaic DP1 (Fig. 5(a)) is limited in distribution throughout the study area and is generally found as 1–3 m diameter ovals of moderately sorted gravel inset with sharp boundaries into other surface mosaics. Finer texture, better sorting, and almost complete coverage (95%) of the soil makes this surface mosaic easy to visually identify. Surface mosaics DP2 (Fig. 5(b)) and DP3 (Fig. 5(c)) are extensive in their distribution, with each comprising about half of all of the planar expanses of desert pavement of the study site. DP2 is differentiated in the field from DP3 by its more thorough cover of the soil (87% *vs*. 69%), closer packing in plan view, smaller clast size (generally medium gravel *vs* coarse gravel), greater angularity, and less firmly embedded nature (Table 1). Those cobble-size clasts of DP2 are generally angular to sub-angular and occasionally dislodged when walked on, whereas those of DP3 are generally sub-angular to subrounded, firmly embedded, and rarely dislodged when walked on.

Bare ground (BG) surface mosaics

Bare ground surface mosaics BG1 (Fig. 5(d)), BG2 (Fig. 5(e)), and BG3 (Fig. 5(f)) are surfaces which visually contrast with desert pavement surface mosaics (Figs. 1

Table 2. *ANOVA results comparing the clast size distributions from multiple one-meter line transects completed on the surface of the e1 flow, Cima volcanic field, east Mojave Desert, California*

Mosaic	Transects, *n*	MS	*F*	df	*p*
Desert pavement					
DP1	3	1·52	0·79	214	0·46
DP2	4	3·55	0·86	196	0·46
DP3	4	16·02	1·58	73	0·20
Bare ground					
BG1	4	37·17	1·85	65	0·15
BG2	4	16·71	2·87	92	0·04
BG3	4	4·19	0·20	33	0·90

Replicate transect data for a specific mosaic type are from significantly different populations of that mosaic type when $p < 0{\cdot}05$.

Table 3. *Mean comparisons between b-axis values for surface mosaic types Comparisons were done within mosaic categories shown by headings*

Mosaic	Mean* (mm)
Between desert pavement mosaics	
DP1	12 (14) b
DP2	21 (25) b
DP3	42 (32) c
Between bare ground mosaics	
BG1	36 (46) ab
BG2	21 (25) b
BG3	47 (44) a

Letters following mean value indicate significant differences between mosaic types based on Tukey's studentized range test (Generalized Linear Model).
*Mean based on combined data from all transects for each mosaic. Standard deviations (±) are shown in parentheses.

and 4). They appear to have abundant bare soil, even though more than 50% of the soil surface may be covered by poorly sorted clasts (Table 1).

The areal distribution of bare ground mosaic BG1 (Fig. 5(d)) is limited across the study site. It is generally found on slopes below bedrock highs and above surface mosaics BG2 and BG3. BG1 is a surface type intermediate in physical character between desert pavement and the other two bare ground surface mosaics (Tables 1 and 3, Fig. 6), and has the greatest range of clast sizes (Table 1). While clasts cover more than half the surface (54%), they are not closely packed to form desert pavement (Fig. 5(d)). The boundaries between BG1 and other surface mosaics are diffuse (Table 1). Many of its angular cobble-size clasts are weakly embedded and often show evidence of past movement. For example, the deposition of calcium carbonate can form a distinctive white 'ring' around clasts at their interface with the soil surface, or a continuous coating within developing clast fractures. On several of the clasts within BG1 these deposits now lie askew in relation to the soil surface (Fig. 5(d)).

Both bare ground mosaics BG2 (Fig. 5(e)) and BG3 (Fig. 5(f)) generally occur as 3–10 m diameter polygons inset into DP2 and DP3 surface mosaics with gradual boundaries (Table 1). These mosaics are generally found on nearly level gradients and have clumps of desert shrubs growing on their surfaces (Fig. 1). In both, subrounded cobble-size clasts are tightly embedded into the soil. However, mosaic BG2 has a unique cover, formed by angular to sub-angular carbonate-encrusted medium and coarse gravel lying free on the surface which easily distinguishes it from the barer BG3 (58% clast cover *vs* 21%).

Spatial consistency of surface mosaic parameters

Cluster analysis of the parameters which define surface mosaics — percent clast cover, sorting index and median clast width — was done using a three-dimensional scatterplot (Data Description, Inc., 1995). This scatterplot was reduced to a two-dimensional representation for publication (Fig. 6) by using the products of sorting index and median clast size as the *y*-axis values, and percent clast cover as the *x*-axis values. Using this cluster analysis, values are graphically constrained for five of the six surface mosaics. Triplicate measurements for the three DP mosaics and for mosaics BG2 and BG3 fall into a unique region of the plot for each specific surface mosaic (Fig. 6). The sixth surface mosaic, BG1 — a visual intergrade between the DP mosaics and the BG2 and BG3 mosaics in the field — has a dispersed distribution of its data across the scatterplot.

An analysis of variance (ANOVA) performed using SAS indicates that the size distributions measured at three sampling locations are drawn from the same population of clasts for the three desert pavement surface mosaics (Table 2). That

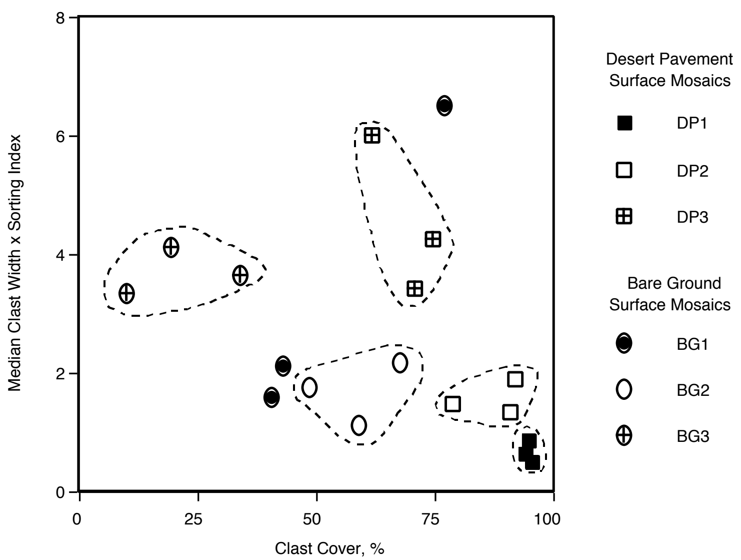

Figure 6. Three-dimension cluster analysis of surface mosaic field data (Data Description, Inc., 1995) which shows separation of defined map units based on measured physical characteristics of (1) percent cover of the soil surface, (2) median clast size, and (3) index of sorting. Since three axes are needed to graph these three parameters, but only two dimensions can be displayed in this figure, the ordinate axis represents the reduction of two of the dimensions. Median clast size and sorting index are represented by the values of their products for each measured meter transect.

is, physical characteristics governed by clast size (mid-point values such as mean and median and the value of sorting) for surface mosaics DP1, DP2, and DP3, are consistent wherever measured on the study site. Tukey's studentized test also shows distinct discrepancies between the size distributions for the three desert pavement surface mosaics based on their means.

However, while ANOVA indicates that surface mosaics BG1 and BG3 are consistent across the studied land form, those size distributions for surface mosaic BG2 are not (Table 2). Tukey's studentized test also shows consistent differences between the size distributions for two of the BG mosaics based on their means. Using this analysis, surface mosaic BG2 and BG3 are distinct from each other, while BG1 is similar to both of them (Table 3).

Discussion

Implications for the study of surficial form and process

The land surface at the field site is readily divided into six surface mosaic types. Statistical analyses of measured desert pavement characteristics show the three DP mosaics to be unique, precise, and consistent across space (Fig. 6, Tables 1–3). These three mosaics each have unique physical characteristics of median clast size, sorting, and percent soil covered by clasts (Fig. 6). Statistical analyses of measured bare ground characteristics indicate that of the three BG mosaics only BG3 is unique (Fig. 6, Tables 1–3). However, the other two BG mosaics are easily distinguished in the field — BG1 by its steeper slopes, carbonate deposits on clasts, and generally larger clast sizes, and BG2 by its distinctive cover of carbonate-encrusted gravel.

These differences in surface physical form translate into differences in surface roughness (Emmet, 1970) which in turn should control rates of fluid flow of wind and water, and associated surface processes such as infiltration, runoff, and sediment deposition and erosion (Yair & Klein, 1973; Dunkerley, 1995). The six surface mosaics abut each other with easily discerned boundaries generally <100 mm wide (Table 1) and form distinct, disjunct regions of surface roughness across the soil surface. Rates of surficial processes are expected to vary across the land surface in disjunct steps in response to these different, readily mapped, surface mosaics.

The distinct differences in surface characteristics between DP mosaics (Table 1) suggest that different processes may be dominant in their formation. For example, the dominant process in the development of surface mosaic DP2 is the pedogenic translocation of eolian sand, silt and salts into underlying soil horizons (Wells *et al.*, 1985, 1995; McFadden *et al.*, 1987; Anderson, 2002). On the other hand, the smaller, better sorted clasts of surface mosaic DP1 appear similar to those described by Haff & Werner (1996) in their study of the regeneration of desert pavement. They cleared clasts from a desert pavement land surface to form square bare ground patches of 100–1600 cm^2. These experimental patches began to infill with fine and medium gravel-size clasts over the monitoring period of 5 years (Haff & Werner, 1996), probably due to hydraulic action (Abrahams *et al.*, 1984). Thus, DP1 surface mosaics may result from previously bare regions of the surface being covered by moderately sorted gravels. Based on the rate of infilling of gravel of 13 cm^2 $year^{-1}$ reported by Haff & Werner (1996), a 3-m diameter patch of DP1 would have required about 5500 years to form under current climatic conditions.

Field reconnaissance of several other arid land surfaces showed that relative textural differences of clast sorting and percent soil cover remain visually consistent with those from this study site. This suggests that this definition of six visually distinct surface mosaics is useful for mapping the spatial heterogeneity of desert pavement formed on other geomorphic surfaces of different ages and depositional origin. The ability to accurately delineate and quantify the physical nature of the clast cover should facilitate study of surficial processes important in the formation and evolution of desert pavement land surfaces.

Implications for multiparameter relative age dating

Relative dating techniques are used to study Quaternary surfaces when no natural material is available for absolute age determinations using radiocarbon dating or other isotopic techniques. The use of rock weathering as a relative dating strategy is based on the premise that certain chemical and physical processes are time-dependent. Thus, with the passage of time, surface clasts will be broken down into smaller pieces, and landforms of different ages, but similar lithologies, can be distinguished based on dissimilar reductions in mean clast size over time (Blackwelder, 1931; Sharp & Birman, 1963; Burke & Birkeland, 1979).

Assessment of rock weathering has been considered a promising strategy for the relative age dating of landforms mantled by desert pavement, since surface clasts can be easily measured to determine mean clast size (McFadden *et al.*, 1989). At this study site, the use of rock weathering would indicate that areas of the e1 basalt flow delineated by mosaics DP1, DP2, and DP3 are all of different relative ages. DP1, with the smallest mean clast diameter, would be considered the oldest, and DP3, with the largest mean clast diameter, the youngest. Instead, mean clast size varied over an order of four even though the studied desert pavement formed on a geomorphic surface of a consistent lithology and a single, known age.

Factors other than differing amounts of time have affected the rate at which surface basalt clasts are broken down into smaller pieces since these clasts are from extruded bedrock of a single age. The initial clast size available to form desert pavement depends on the underlying sedimentary unit. At this field site, the geochemical nature of the cooling basalt produced a preferential fragment size of at least cobbles, based on the maximum clast size data from Table 1. Over time this initial size has been broken down into regions of distinct size categories with means ranging from medium to coarse gravel.

Presently, the spatially disjunct fabric and texture of the six different surface mosaics partition process across this land surface. These spatially unique size distributions of clasts must reflect and cause differences in surface processes. That is, the entrapment of eolian dust, the infiltration of water, and the translocation of salts and clays into the soil occur at rates governed by the physical nature of the clast cover. As these rates vary discretely at a scale of meters, so does the evolution of the near-surface soil and clast cover. Where clast cover is high, reduced rates of infiltration associated with increased concentrations of near-surface salts would foster the physical breakdown of surface clasts by salt fracturing. Over time, these processes would lead to smaller surface clast size and increased clast cover in some regions of the study site. In contrast, where clast cover is decreased, higher infiltration rates would carry salts deeper into the soil, thus decreasing rates of clast breakdown to smaller sizes. Large-scale patterning of the land surface, and accompanying processes, must be taken into account when using rock weathering as a relative-age dating technique of desert pavement-covered landforms.

This research was supported in part by an Academic Senate Travel Grant from the University of California and as fellowship monies from the Desert Research Institute, the Desert Studies Consortium, as well as the Graduate Division of the University of California. Special thanks are given to Thérèse and Marc Mercier, April Ulery, Marcella Waggoner, Tanja Williamson, and Skipper Wood for invaluable assistance in the field. Many thanks are sent to the staff of the

Zzyzx Research Station for support in the form of lodging and computer facilities, and to the National Park Services for approval to conduct research on their land.

References

Abrahams, A.D. & Parsons, A.J. (1991). Relation between infiltration and stone cover on a semiarid hillslope, southern Arizona. *Journal of Hydrology*, **122**: 49–59.

Abrahams, A.D., Parsons, A.J., Cooke, R.U. & Reeves, R.W. (1984). Stone movement on hillslopes in the Mojave Desert, California: a 16-year record. *Earth Surface Processes and Landforms*, **9**: 365–370.

Anderson, K.C., Wells, S.G., & Graham, R.C. (2002). Pedogenesis of vesicular horizons, Cima volcanic field, Mojave Desert, California. *Soil Science Society of America Journal*, (in press).

Arvidson, R.E., Shepard, M.K., Guinness, E.A., Petroy, S.B., Plaut, J.J., Evans, D.L., Farr, T.G., Greeley, R., Lancaster, N. & Gaddis, L.R. (1993). Characterization of lava-flow degradation in the Pisgah and Cima volcanic fields, California, using Landsat Thematic Mapper and AIRSAT data. *Geological Society of America Bulletin*, **105**: 175–188.

Billings, W.D. (1949). The shadscale vegetation zone of Nevada and eastern California in relation to climate and soils. *American Midlands Naturalist*, **42**: 87–109.

Blackwelder, E. (1931). Pleistocene glaciation in the Sierra Nevada and Basin Ranges. *Geological Society of America Bulletin*, **42**: 865–892.

Burke, R.M. & Birkeland, P.W. (1979). Reevaluation of multiparameter relative dating techniques and their application to the glacial sequence along the eastern escarpment of the Sierra Nevada, California. *Quaternary Research*, **11**: 21–51.

Compton, R. R. (1985). *Geology in the Field*. New York, NY: John Wiley and Sons. 398 pp.

Cooke, R.U. (1965). Desert pavement. *Mineral Information Service*, **18**: 197–200.

Cooke, R.U. (1970). Stone pavements in deserts. *Association of American Geographers Annals*, **60**: 560–577.

Cooke, R.U., Warren, A. & Goudie, A. (1993). *Desert Geomorphology.* London: UCL Press, Ltd. 526 pp.

Data Description, Inc. 1995. *DataDesk 5·0: Exploratory Data Analysis.* Ithaca, NY: Data Description, Inc. 575 pp.

Denny, C.S. (1965). Alluvial fans in the Death Valley regions, California and Nevada. *United States Geological Survey Professional Paper 288*.

Dohrenwend, J.C., Abrahams, A.D. & Turrin, B.D. (1987). Drainage development on basaltic lava flows, Cima volcanic field, southeast California, and Lunar Crater volcanic field, south-central Nevada. *Geological Society of America Bulletin*, **99**: 405–413.

Dohrenwend, J.C., McFadden, L.D., Turrin, B.D. & Wells, S.G. (1984). K–Ar dating of the Cima volcanic field, eastern Mojave Desert, California: Late Cenozoic volcanic history and landscape evolution. *Geology*, **12**: 163–167.

Dunkerley, D.L. (1995). Surface stone cover on desert hillslopes: parameterizing characteristics relevant to infiltration and surface runoff. *Earth Surface Processes and Landforms*, **20**: 207–218.

Dunkerley, D.L. & Brown, K.J. (1995). Runoff and runon areas in a patterned chenopod shrubland, arid western New South Wales, Australia: characteristics and origin. *Journal of Arid Environments*, **30**: 41–55.

Emmet, W.W. (1970). The hydraulics of overland flow on hillslopes. *United States Geological Survey Professional Paper 662-A*.

Evenari, M. (1985). The desert environment. In: Evenari, M., Noy-Meir, I. & Goodall, D.W. (Eds), *Hot Deserts and Arid Shrublands, Part A*, pp. 1–22. New York, NY: Elsevier Science Publishing Company. 365 pp.

Farr, T.G. (1992). Microtopographic evolution of lava flows at Cima Volcanic Field, Mojave Desert, California. *Journal of Geophysical Research*, **97**: 15,171–115, 179.

Folk, R.L. (1980). *Petrology of Sedimentary Rocks*. Austin, TX: Hemphill Publishing Company. 182 pp.

Haff, P.K. & Werner, B.T. (1996). Dynamical processes on desert pavements and the healing of surficial disturbances. *Quaternary Research*, **45**: 38–46.

Hunt, C.B. & Mabey, D.R. (1966). Stratigraphy and structure. Death Valley, California. *United States Geological Survey Professional Paper 494-A*.

Jackson, E.A. (1957). Soil features in arid regions with particular reference to Australia. *Journal of the Australian Institute of Agricultural Science*, **25**: 196–208.
Ludwig, J.A., Cunningham, G.L. & Whitson, F.D. (1988). Distribution of annual plants in North American deserts. *Journal of Arid Environments*, **15**: 221–227.
McFadden, L.D., Ritter, J.B. & Wells, S.G. (1989). Use of multiparameter relative-age methods for age estimation and correlation of alluvial fan surfaces on a desert piedmont, Eastern Mojave Desert, California. *Quaternary Research*, **32**: 276–290.
McFadden, L.D., Wells, S.G. & Dohrenwend, J.C. (1986). Influences of Quaternary climatic changes on processes of soil development on desert loess deposits of the Cima volcanic field, California. *Catena*, **13**: 361–389.
McFadden, L.D., Wells, S.G. & Jercinovich, M. (1987). Influences of eolian and pedogenic processes on the origin and evolution of desert pavements. *Geology*, **15**: 504–508.
McFadden, L.D., McDonald, E.V., Wells, S.G., Anderson, K., Quade, J., & Forman, S.L. (1998). The vesicular layer and carbonate collars of desert soils and pavements: formation, age and relation to climate change. *Geomorphology*, **24**: 101–145.
Nettleton, W.D. & F.F. Peterson (1983). Aridisols. In: Wilding, L.P., Smeck, N.E. & Hall, G.F. (Eds), *Pedogenesis and Soil Taxonomy. II. The Soil Orders*, pp. 165–215. Amsterdam: Elsevier Science Publishers. 410 pp.
NOAA (1999). Climatological data annual summary, California. Volume 103, Number 13. Environmental Data and Information Service, National Oceanic and Atmospheric Administration, United States Department of Commerce.
Schoeneberger, P.J., Wysocki, D.A., Benham, E.C. & Broderson, W.D. (1998). *Field Book for Describing and Sampling Soils*. Lincoln, NE: National Soils Survey Center, National Resources Conservation Service, USDA.
Sharp, R.P. & Birman, J.H. (1963). Additions to classical sequence of Pleistocene glaciations, Sierra Nevada, California. *Geological Society of America Bulletin*, **74**: 1079–1086.
Smith, S.D., Herr, C.A., Leary, K.L. & Piorkowski, J.M. (1995). Soil-plant water relations in a Mojave Desert mixed shrub community: a comparison of three geomorphic surfaces. *Journal of Arid Environments*, **29**: 339–351.
Springer, M.E. (1958). Desert pavement and vesicular layer of some soils of the desert of the Lahontan basin, Nevada. *Soil Science Society of America Proceedings*, **22**: 63–66.
Turrin, B.D., Dohrenwend, J.C., Drake, R.E. & Curtis, G.H. (1985). K–Ar ages from the Cima volcanic field, eastern Mojave Desert, California. *Isochron West*, **44**: 9–16.
Vasek, F.C. & Barbour, M.G. (1988). Mojave desert scrub vegetation. In: Barbour, M.G. & Major, J. (Eds), *Terrestrial Vegetation of California*, pp. 835–867. Davis, CA: California Native Plant Society. 1013 pp.
Wells, S.G., Dohrenwend, J.C., McFadden, L.D., Turrin, B.D. & Mahrer, K.D. (1985). Late Cenozoic landscape evolution of lava flow surfaces of the Cima Volcanic Field, Mojave Desert, California. *Geological Society of America Bulletin*, **96**: 1518–1529.
Wells, S.G., McFadden, L.D., Poths, J. & Olinger, C.T. (1995). Cosmogenic 3He surface-exposure dating of stone pavements: implications for landscape evolution in deserts. *Geology*, **23**: 613–616.
Whalley, W.B. (1983). Desert varnish. In: Goudie, A.S. & Pye, K. (Eds), *Chemical Sediments and Geomorphology*, 179–229. London: Academic Press.
Yair, A. & Klein, M. (1973). The influence of surface properties on flow and erosion processes on debris covered slopes in an arid area. *Catena*, **1**: 1–18.